Challenges for Structural Health Monitoring: Nonlinearities and Uncertainties

Luis Gustavo Giacon Villani, Sidney Bruce Shiki, Americo Cunha Jr, Samuel da Silva, Michael D. Todd

Challenges for Structural Health Monitoring: Nonlinearities and Uncertainties

Luis G. G. Villani[1*], Sidney B. Shiki[2], Americo Cunha Jr[3], Samuel da Silva[4*] and Michael D. Todd[5]

[1]Universidade Federal do Espirito Santo (UFES), Brazil. e-mail: luis.villani@ufes.br
[2]Universidade Federal de São Carlos (UFSCar),Brazil, bruce@ufscar.br
[3]Universidade do Estado do Rio de Janeiro (UERJ), Brazil, americo@ime.uerj.br
[4*]Universidade Estadual Paulista (UNESP), Brazil, samuel.silva13@unesp.br
[5]University California San Diego, EUA, mdtodd@eng.ucsd.edu

[*]samuel.silva13@unesp.br

Abstract

Implementing structural health monitoring (SHM) techniques with a high Technology Readiness Level (TRL) is still challenging due to several practical requirements and assumptions to apply the fundamental methods. Between them, two issues earn some special attention: the linearity hypothesis and the robustness to the natural variability of data. The first point to overcome is that many structural engineering systems inherently behave nonlinearly during operation, even in a healthy state. Here, the assumption of linearity is typically inaccurate, eliminating large classes of feature extraction techniques. This issue is more complicated when the Damage also induces additional nonlinearities, e.g., cracking. The second aspect is the need to quantify the parameters' variation and uncertainties and signal data to interrogate the structural state. This chapter proposes introducing these challenges and some examples of addressing them in this context.

Keywords: nonlinearities; uncertainty quantification; damage detection

1 Introduction

Implementing a Structural Health Monitoring (SHM) strategy is essential to avoid and prevent catastrophic failures in civil, mechanical, and aeronautical systems. Different paradigms utilize physics-based methods (numerical models coupled with model updating, for example) and data-driven methods (where models or trends are inferred from the data alone). Regardless of approach, SHM requires sensors to be deployed on the structure to measure raw information from which it is necessary to extract features sensitive to whatever target Damage mechanisms are of interest. These features are then subject to some sort of classification or discrimination process to make informed decisions about the state of the Damage. Damage is a mechanism that modifies the properties of mass, damping, stiffness, connectivity, or boundary conditions, individually or mutually, that prevent the structure from performing its intended design functions. The primary issue is that the variation observed in these properties can be caused by several different sources, not necessarily only by the presence of Damage. This is a lack of *specificity*. Furthermore, data itself contains many sources of noise that corrupt the measurements and propagate the error into the features and the decision space; this leads to a lack of *sensitivity*. These combined challenges of specificity and sensitivity are problematic for practical, long-term SHM applications, reducing its potential performance.

Among all practical limitations, this chapter focuses on two issues that may decrease the performance of an SHM method, which we have been investigating for the last ten years. The first is the inherent nonlinear behavior of the vibration motion of flexible and light structures. A nonlinear behavior that leads to the breaking of the superposition principle can be induced when a linear system is subjected to the presence of some types of Damage. That is the case when a crack is presented in a simple clamped-free beam when the level of force excitation is low. When the Damage is propagated, a breathing crack causes a bilinear effect that violates the system's linearity and manifests in the data vibration. Modern engineering systems are manufactured with advanced materials, which demands constitutive equations that are more complex than traditional ones breaking the assumptions of linearity even in a healthy state. Consequently, an algorithm of SHM is required to separate the nonlinear effects induced by damaged from the inherent nonlinearities.

The second challenge to overcome is the presence of uncertainties in structure monitoring. The measured data may include heavy noise and systemic uncertainties caused by boundary condition variations, property change not caused by Damage, variation in the parameters caused by temperature changes, etc. Consequently, the features extracted from measured signals can be corrupted to compute the damage indices. On the other hand, the models built to monitor the structures are also full of uncertainties in the definition of their parameters and the assumptions and simplifications adopted throughout the modeling. Therefore, to ensure statistical reliability in the results obtained, such uncertainties must be considered in the construction and testing stage of the methodologies.

Both limitations severely harm damage detection because they can increase the level of false alarms and reduce the reliability of the diagnosis. It is essential to simultaneously develop and apply an SHM methodology to deal with these concerns. The key idea to get around these problems is to choose features that are insensitive to these variations, use projections and transformations, or use extensive data for learning purposes, increasing the amount of available measured data. Unfortunately, both options can be problematic and non-trivial to be quickly implemented. This chapter introduces these challenges by exploiting two benchmarks examples in simple beam structures with nonlinear behavior and uncertainties. Data of both setups are shared to allow the reader to deal with methods to observe the effects of nonlinearities and uncertainties in the performance degradation of the SHM algorithms.

Section 2 introduces general concepts of uncertainty quantification (UQ) and demonstrates how these natural variabilities can harm the damage-sensitive features used in traditional SHM algorithms. Section 3 illustrates a general approach for integrating the assumptions and concepts of uncertainty quantification and nonlinear system identification in damage detection for SHM purposes in nonlinear systems. First, the section presents an overview of data-driven modeling and system identification (ID) to detect and understand, based on data, the systems' nonlinear behavior. Many different ID models could be chosen, but a nonparametric approach based on the Volterra series is selected because this series is a straightforward generalization of the convolution concept of linear systems and strongly correlates with the frequency response functions for higher-order components. Section 4 provides two examples of applying the described methodology using experimental data. Firstly, under conditions where a deterministic model is enough to guarantee the detection of structural variations, where the variability of the data is small. And then a more interesting experiment, involving a more significant data variability, where the stochastic approach is needed to ensure good performance (closer to the real world). Finally, the Section 5 provides the main conclusions and propositions for future work.

2 Overview in Uncertainty Quantification (UQ) and its relevance to SHM

2.1 General definitions

The uncertainties can be classified into two main groups [Soize, 2012, 2017]:

- **Data uncertainties:** also known as *aleatory*, these uncertainties are intrinsic to scenarios with variabilities, such as noise in the measured data (experimental data) and variations concerning the nominal configuration of the structures, due to geometric imperfections, manufacturing irregularities, environmental conditions, etc. These uncertainties can not be eliminated, only better characterized;

- **Model uncertainties:** also known as *epistemic*, these uncertainties result from the limited knowledge about the model structure to be used, i.e., ignorance about the system's physics. These uncertainties can be mitigated or even eliminated by increasing knowledge about the behavior of the system in analysis.

Dealing with model uncertainty is no simple task. Although they can be reduced as the models are improved, it is practically impossible to build models that are totally faithful to the physical phenomena involved. In this case, it is interesting that the model can provide some level of information about the uncertainties involved in its own prediction estimation process. Physical models encounter great difficulty in performing this kind of estimation, which is much more common when considering machine learning-based models. In the context of this work, we assume that model uncertainties can be neglected, although we know that in reality, they will be present. This simplification is made by assuming that the chosen baseline nonlinear model (the Volterra series) is efficient enough to describe the phenomena under study, so those model uncertainties will not have much influence on the final result. The results obtained experimentally support this belief.

On the other hand, as mentioned, data uncertainties cannot be eliminated, but they can be better characterized. A better characterization of this type of uncertainty can give the model the ability to predict the behavior of the dynamic systems under study with a certain level of statistical reliability. When dealing with experiments where data variability can be significant (almost all real-world applications), this capability can improve the performance of the monitoring metrics adopted. The most usual way to consider data uncertainties in estimating a numerical model is to apply a parametric probabilistic approach [Soize, 2017], that considers the model parameters sensitive to the presence of uncertainties as random objects (such as random variables, random vectors or random processes). After characterizing the joint-distribution of these parameters, the underlying uncertainties can be propagated through the model using the well-known Monte Carlo (MC) method, and statistics of the model output can be obtained. Experimental applications will make clearer the advantage of adopting this kind of approach when estimating stochastic models in the context of damage detection.

2.2 The problem of data variation in the context of SHM

As mentioned before, in the context of SHM, the presence of data variation can confuse the deterministic metrics, as shown in Villani et al. [2019b], being the use of probabilistic models necessary to improve the results. Figure 1 highlights how the data variation can complicate the implementation of classical SHM methodologies. Modal parameters are standard features to consider in the damage detection problem because Damage induces variations in structural properties, which are reflected in the vibration modes of the structures. It is interesting to observe that depending on the level of data variation in the measured signals and extension of the Damage, it is difficult to observe the presence of Damage when the modal parameters are used as the damage-sensitive feature. There is a superposition between the features calculated on reference condition and under damage I condition. Therefore, if we use the modal parameters directly as damage indicators in a deterministic approach or even using powerful machine learning algorithms, we will not be able to detect damage condition I, under these circumstances. The details about the data can be found in Villani et al. [2019c].

When dealing with data analysis directly (data-based monitoring), it is possible to project these features in dimensions where the variability of the measured data is reduced or try to compensate the variability using a reference parameter, the temperature, for example. It is also possible to extract features from the signals that may be less influenced by data variability and implement more powerful classification algorithms. However, when dealing with SHM based on prediction models, as is the case where nonlinear behavior is involved, some statistical certification for the model is always necessary because the presence of uncertainties also influences the parameters of the models. Therefore, these uncertainties must be characterized and incorporated into the model identification step to build stochastic models capable of performing the prediction with statistical reliability.

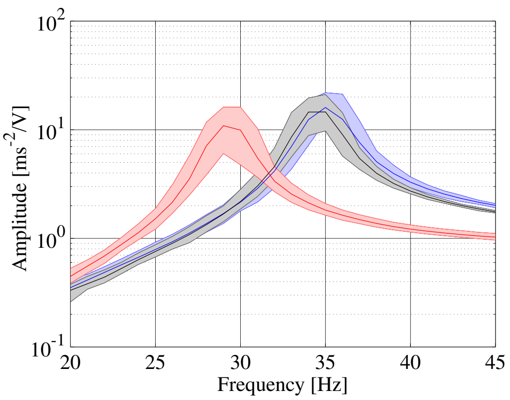

(a) FRF, where the continuous lines represent the mean values and the color zones the curves obtained with 99% of confidence, - reference, - damage I and - damage II.

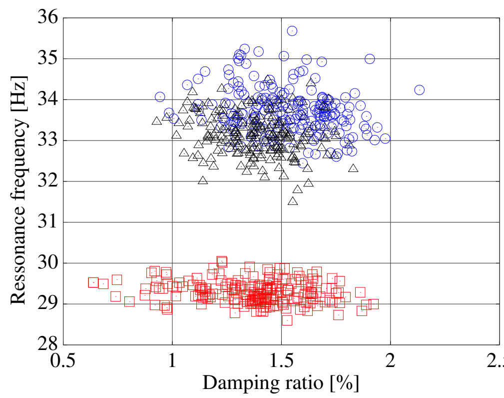

(b) Variation of linear modal parameters. ○ - reference, △ - damage I and □ - damage II.

Figure 1: Uncertainties induced by variations in the measured data.

3 An integrated SHM approach using Nonlinearities and UQ

3.1 Nonlinear system identification

There are two main ways to handle the presence of nonlinear phenomena in SHM problems [Nichols and Todd, 2009]:

- **The healthy structures present linear behavior:** Damage induces the linear structure to present nonlinear phenomena in its behavior. The Damage can be detected by observing nonlinear behavior in the measured systems' output signals. When we want to achieve higher steps of SHM, usually, a nonlinear model is necessary to predict the structure's output signals in damaged conditions. Many works were developed in this sense, aiming to detect delaminations [Ghrib et al., 2018], breathing cracks [Rébillat et al., 2014], unbalance in rotor systems [Xia et al., 2016], and others;

- **The structures present nonlinear behavior even in healthy conditions:** the structure presents nonlinear phenomena in its output signal in the reference condition, and this behavior can be confused with damages when the approaches described previously are applied [Bornn et al., 2010]. This situation makes necessary the use of more sophisticated methods that can differentiate the effects caused by the damages and the ones caused by the inherent nonlinearities.

The second scenario is more critical. Figure 2 shows an example of the situation described; the data used was measured considering a magneto-elastic nonlinear structure exposed to the presence of a structural change that emulates the behavior of a breathing crack. The presence of multiple harmonics in the responses suggests nonlinear oscillatory behavior. The structure presents linear behavior when a low energy level is applied; however, when high amplitudes are achieved, it manifests nonlinear phenomena. Moreover, the structure is exposed to the presence of a breathing crack that induces nonlinear behavior. When dealing with the second scenario, the construction of a model capable of predicting the intrinsically nonlinear behavior of the system and providing information that allows differentiating the intrinsic phenomena of the system from that caused by Damage is of great relevance. Many nonlinear models could be proposed to solve this issue, and the reader is invited to see Kerschen et al. [2007], Worden et al. [2007] for exploring this vast universe.

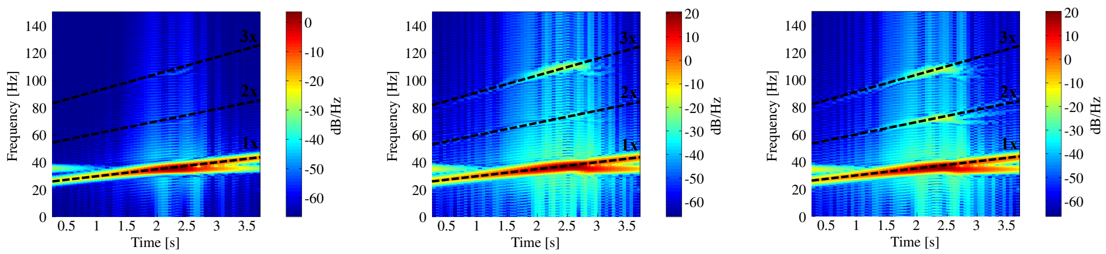

(a) Reference - low amplitude. (b) Reference - high amplitude. (c) Damaged - high amplitude.

Figure 2: Time-frequency diagram of the system's output exemplifying the presence of nonlinear phenomena.

The authors decided to use the Volterra series nonlinear data-driven model for dealing with the intrinsically nonlinear behavior of such systems. The choice is based on the capability of the Volterra series to separate linear and nonlinear contributions to the predicted response since this model represents a generalization of the linear convolution concept.

Consider a discrete-time causal nonlinear system with a single output $k \in \mathbb{Z}_+ \mapsto y(k)$ caused by a single input $k \in \mathbb{Z}_+ \mapsto u(k)$, with $\mathbb{Z}_+$ representing the set of nonnegative integers. Through the discrete-time Volterra series, nonlinear system's output can be written in the form

$$y(k) = \sum_{\eta=1}^{\infty} \sum_{n_1=1}^{N_1} \cdots \sum_{n_\eta=1}^{N_\eta} \mathcal{H}_\eta(n_1, \ldots, n_\eta) \prod_{i=1}^{\eta} u(k - n_i) = \underbrace{y_1(k)}_{linear} + \underbrace{y_2(k) + \cdots + y_\eta(k)}_{nonlinear}, \quad (1)$$

where $(n_1, .., n_\eta) \in \mathbb{Z}_+^\eta \mapsto \mathcal{H}_\eta(n_1, \ldots, n_\eta)$ represents the η-order Volterra kernel, N the number of input lags considered in each kernel, and $k \in \mathbb{Z}_+ \mapsto \{y_1(k), y_2(k), \ldots, y_\eta(k)\}$ represent, respectively, the first kernel (linear) contribution, the second kernel (quadratic) contribution, and the η-order kernel contribution [Schetzen, 1980].

The main disadvantage of the approach is the challenge in achieving the convergence when a high number of terms is used [Shiki et al., 2017, Villani et al., 2019a]. In order to reduce the number of terms necessary to obtain a good approximation, the Volterra kernels $\mathcal{H}_\eta$ can be expanded into an orthonormal basis, such as the Kautz functions [Kautz, 1954]. In this way, the series can be rewritten according to the approximation

$$y(k) \approx \sum_{\eta=1}^{\infty} \sum_{i_1=1}^{J_1} \ldots \sum_{i_\eta=1}^{J_\eta} \mathcal{B}_\eta \left(i_1, \ldots, i_\eta\right) \prod_{j=1}^{\eta} l_{\eta,i_j}(k) \,, \tag{2}$$

where J represents the number of Kautz functions used in each orthonormal projections of the Volterra kernels, $(i_1, \ldots, i_\eta) \in \mathbb{Z}_+^\eta \mapsto \mathcal{B}_\eta(i_1, \ldots, i_\eta)$ represents the η-order Volterra kernel expanded in the orthonormal basis, $k \in \mathbb{Z}_+ \mapsto l_{\eta,i_j}(k)$ is a simple filtering of the input signal $u(k)$ by the Kautz function ψ_{η,i_j} related to each kernel. Information about the Kautz functions can be found in da Silva et al. [2010]. The kernels' coefficients can be estimated using linear regression algorithms, such as the least-squares method [Shiki et al., 2017].

The classical version of the Volterra series expanded using Kautz filters is a useful deterministic nonlinear model. However, as mentioned before, practical applications involving real-world data deal with the presence of uncertainties. If the experimental data present small variability, related to a low level of noise in the measurements, the deterministic version of the model is sufficient to monitor the system, on the other hand, if the data present high variability, related to noise and operational conditions, the model can be rewritten to take into account *data uncertainties*. The *model uncertainties* are not considered here, which means that we assume that the nonlinear model is able to describe the nonlinearities considered in the analysis performed. A parametric probabilistic approach is employed, meaning that the model parameters subjected to uncertainties are described as random variables or random processes [Soize, 2017]. The stochastic version of the Volterra-Kautz model can be described as

$$\mathrm{y}(\theta, k) \approx \sum_{\eta=1}^{\infty} \sum_{i_1=1}^{J_1} \ldots \sum_{i_\eta=1}^{J_\eta} \mathbb{B}_\eta \left(\theta, i_1, \ldots, i_\eta\right) \prod_{j=1}^{\eta} \mathbb{l}_{\eta,i_j}(\theta, k) \,, \tag{3}$$

where, in this new version, the random process $(\theta, k) \in \Theta \times \mathbb{Z}_+ \mapsto \mathrm{y}(\theta, k)$ represents the stochastic nonlinear system's output, $(\theta, n_1, .., n_\eta) \in \Theta \times \mathbb{Z}_+^\eta \mapsto \mathbb{B}_\eta\left(\theta, i_1, \ldots, i_\eta\right)$ represents the random version of the η-order Volterra kernel expanded in the Kautz basis, and the random process $(\theta, k) \in \Theta \times \mathbb{Z}_+ \mapsto \mathbb{l}_{i_j}(\theta, k)$ is a simple filtering of the deterministic input signal $u(k)$ by the random Kautz function Ψ_{η,i_j}, i.e.,

$$\mathbb{l}_{\eta,i_j}(\theta, k) = \sum_{n_i=0}^{J_\eta} \Psi_{\eta,i_j}(\theta, n_i) u(k - n_i). \tag{4}$$

Estimating the random kernels (the random coefficients) can be done based on the deterministic method described before and Monte Carlo simulations [Kroese et al., 2011, Cunha Jr et al., 2014]. Since we have the random kernels computed when a new input signal is applied, the output signal can be obtained using the uncertainty propagation through the model (again implementing

Monte Carlo simulations). The stochastic model is versatile and can be used to describe a variety of polynomial nonlinearities, considering data variation. Additionally, the component filtering characteristic of the model enables the comparison between the use of linear and nonlinear metrics and the extraction of nonlinear features sensitive to the presence of nonlinear behavior induced by Damage. More details can be obtained in Villani et al. [2019c].

3.2 Extraction of features sensitive to Damage

With the method described in the previous section, it is possible to identify a model representing a structural system's linear and nonlinear dynamics. One can use the discrepancies detected in a measured output y_{exp} concerning the Volterra series considering η terms in the expansion described in Eq. 1. The η-th order prediction error can then be defined by

$$e_{\eta} = y_{exp} - \sum_{m=1}^{\eta} y_m \,. \tag{5}$$

It is expected that the prediction error presents an important change in its statistical properties when the system is subjected to damage. To summarize the deviation of a structure in an unknown structural state, a λ_{η} damage index is applied

$$\lambda_{\eta} = \frac{\sigma\left(e_{\eta,unk}\right)}{\sigma\left(e_{\eta,ref}\right)} \,, \tag{6}$$

where σ denotes the sample standard deviation, $e_{\eta,unk}$ and $e_{\eta,ref}$ are the prediction errors measured in an unknown structural condition and the baseline state, respectively. This index is similar to the one used in the article of Sohn and Farrar [2001] used to detect nonlinear Damage in an initially linear system. A pure linear dynamics can represent the λ_{η} index for $\eta = 1$ in the case where the Volterra expansion matches a simple linear convolution [Peng et al., 2021], or it can take into account higher-order contributions of the Volterra series expansion for $\eta > 1$. This property is used in the present chapter to evaluate possible issues that might appear when using linear models to represent and monitor inherently nonlinear structures.

It is worth mentioning that the features described above make use of the deterministic version of the Volterra series model and are very effective for applications where the uncertainties have low influence, as will be demonstrated in the experimental example. When dealing with a higher level of variability, such features can fail in detecting the variations only related to the presence of Damage, and new features should be determined, considering the nonlinear stochastic model.

Let's assume that the first three kernels are enough to describe the nonlinearity of the monitored system. The stochastic model represented by Eq. 3 can be estimated with the system operating under healthy conditions. This model provides a family of models, through MC simulations, that represent the mechanical system in the reference state. This family of models can be used to formulate a new damage index, stochastic in this case, as follows

$$\mathbb{I}_{lin} = [\Lambda_{lin}(\theta, i_1) \;\; \mathbb{C}_{lin}(\theta, n_{pca})]_{(N_s \times (J_1 + n_{pca}))} \,, \tag{7}$$

for the linear components, and

$$\begin{aligned} \mathbb{I}_{nlin} = [\Lambda_{qua}(\theta, i_1 = i_2) \;\; \Lambda_{cub}(\theta, i_1 = i_2 = i_3) \;\ldots \\ \ldots \;\mathbb{C}_{qua}(\theta, n_{pca}) \; \mathbb{C}_{cub}(\theta, n_{pca})]_{(N_s \times (J_2 + J_3 + 2n_{pca}))} \,, \end{aligned} \tag{8}$$

for the nonlinenar ones, where N_s represents the number of MC simulations used. These indices take into account the identified coefficients of each kernel $\{\Lambda_{lin}(\theta, i_1),\ \Lambda_{qua}(\theta, i_1 = i_2)$ and $\Lambda_{cub}(\theta, i_1 = i_2 = i_3)\}$ and the principal components of the contributions of each kernel to the total output calculated using the stochastic model

$$
\begin{aligned}
\mathbb{y}_{lin}(\theta, k) &\gg \text{PCA} \gg \mathbb{C}_{lin}(\theta, 1), \ldots, \mathbb{C}_{lin}(\theta, n_{pca}), \\
\mathbb{y}_{qua}(\theta, k) &\gg \text{PCA} \gg \mathbb{C}_{qua}(\theta, 1), \ldots, \mathbb{C}_{qua}(\theta, n_{pca}), \\
\mathbb{y}_{cub}(\theta, k) &\gg \text{PCA} \gg \mathbb{C}_{cub}(\theta, 1), \ldots, \mathbb{C}_{cub}(\theta, n_{pca}),
\end{aligned}
\tag{9}
$$

where n_{pca} represents the number of principal components to be used. This is a brief description and more information about the mathematical formulation can be found in Villani et al. [2019c]. The main advantage here is that the damage index in the reference condition takes into account the natural variability of the experimental data, reducing the probability of false positives in the analysis while separating out the effect of nonlinearities in the system dynamics. When the mechanical system operates in an unknown condition a new index can be calculated and compared with this reference stochastic model using supervised methods, described below.

3.3 Classification of structural states by using supervised methods

For the index calculated using Eq. 6, a simple outlier analysis using thresholds is enough to differentiate the damage states from the reference condition because the index is uni-dimensional. For doing so, simply define a theoretical distribution to represent the index in the reference condition and use the probability measures of false alarms to define the threshold value.

However, for the stochastic indices (Eqs. 7 and 8), this direct procedure is not possible. There are several ways to approach multivariate data classification. One simple and effective way is to use metrics based on distance measures to generate a uni-dimensional index that can also be represented by a theoretical distribution. In this sense, the Mahalanobis distance can be used

$$
\mathcal{D}_m^2 = [\mathcal{I}_m - \mu_{\mathbb{I}_m}]^{\mathrm{T}}\, \Sigma_{\mathbb{I}_m}^{-1}\, [\mathcal{I}_m - \mu_{\mathbb{I}_m}]\,,
\tag{10}
$$

where the sub-index m represents both linear and nonlinear features, $\Sigma_{\mathbb{I}_m}$ and $\mu_{\mathbb{I}_m}$ are the covariance matrix and the mean vector of the feature vector completed considering the reference condition (using Eqs. 7 and 8), and $\mathcal{I}_m$ represents the index vector calculated with the mechanical system in an unknown condition. This metric calculates the distance between $\mathcal{I}_m$ and the mean of $\mathbb{I}_m$ taken into account the dispersion and correlation of $\mathbb{I}_m$. Now, a theoretical probability distribution can be proposed for $\mathcal{D}_m^2$ and an outlier analysis can be implemented through threshold definition.

It is worth mentioning that different machine learning methods could be used to monitor the structural condition through the proposed damage indices. The choice depends on the ability to separate the data for the features. Since the features calculated here can remarkably separate the different conditions, a simple outlier analysis using one-dimensional metrics is enough to detect the occurrence of Damage. For states considering more incipient Damage, more robust methods may be needed.

3.4 Definition of thresholds: statistical approaches for hypothesis tests

By considering the deterministic approach with the λ_η index (Eq. 6), it is possible to define a statistical methodology assuming that the prediction errors have a Gaussian distribution [Shiki et al., 2017]. With this, the λ_η indicator can be related to a F distribution which describes the ratio between the variances of two random variables [Bendat and Piersol, 2011]. In this sense, the expected probability density function $P(\lambda)$ is given by

$$P(\lambda) = \frac{2\left[\frac{v_1}{v_2}\right]^{\frac{v_1}{2}} \lambda^{v_1 - 1}}{\beta\left(\frac{v_1}{2}, \frac{v_2}{2}\right)\left[1 + \frac{v_1}{v_2}\lambda^2\right]^{\left(\frac{v_1+v_2}{2}\right)}}, \tag{11}$$

where v_1 and v_2 are the number of degrees of freedom for the prediction errors in the unknown and reference conditions respectively and β is the function:

$$\beta(a_1, a_2) = \frac{(a_1 - 1)!\,(a_2 - 1)!}{(a_1 + a_2 - 1)!}, \tag{12}$$

where a_1 and a_2 are the input arguments of the β function. In this sense, using the deterministic version of the Volterra series, the damage detection process can be summarized by a statistical hypothesis test to detect a significant increase in the prediction error under a significance level α:

$$\begin{cases} H_0 : \sigma(e_{\eta,unk}) = \sigma(e_{\eta,ref})\ , \\ H_1 : \sigma(e_{\eta,unk}) > \sigma(e_{\eta,ref})\ , \end{cases} \tag{13}$$

where H_0 is the null hypothesis which represents the condition where it is likely that the system is still in the reference condition, and H_1 is the alternative hypothesis that represents the case where the standard deviation presented a significant increase due to some modification in the system behavior. This means that in this formulation, it is considered that no other effects are changing the system's response (e.g., environmental variations or uncertainties effects).

When using the Mahalanobis distance calculated (Eq. 10) it is necessary to propose a new hypothesis test. In this regard, we can assume that the Mahalanobis distance can be described by a chi-square distribution when calculated in the reference condition. Within that assumption, we need to ensure the premise of independence and normality in the underlying multivariate features used to calculate the distance measure [Yeager et al., 2019]. Therefore, by integrating the chi-square PDF, we can calculate the probability of a new distance value to belong the theoretical distribution [Grimmett and Welsh, 2014]

$$p_m = F(\mathcal{D}_m^2|\nu) = \int_0^{\mathcal{D}_m^2} \frac{t^{(\nu-2)/2} e^{-t/2}}{2^{\nu/2}\Gamma(\nu/2)} dt\,, \tag{14}$$

where p_m is the probability of the value $\mathcal{D}_m^2$ belonging to the chi-square distribution, ν is the number of degrees-of-freedom, and $\Gamma(.)$ is the Gamma function.

At last, we can propose a probability threshold value to decide if the sample belongs or not to the theoretical distribution. This sensitivity value depends on the probability of false alarms tolerated in the specific application. At this point, the hypothesis test can be rewritten

$$\begin{cases} H_0 : p_m \geq \epsilon\,, \\ H_1 : p_m < \epsilon\,, \end{cases} \tag{15}$$

where ϵ represents the value of sensitivity chosen. The definition of α and ϵ depends on the practical application and for laboratory studies, various values can be examined to test the performance of the methods.

3.5 Probability of false alarm and ROC curve

With the statistical procedure presented in the subsection 3.4, it is possible to accept or reject the null hypothesis, which can give an insight into the structural state of the dynamic system. The threshold for this binary classification is governed by the significance level of the hypothesis test.

The performance of this classification can be carried out by evaluating the false alarm rate, which represents the number of false positives indicated by a damage index, against the true detection rate, which reflects the sensitivity of the proposed methodology. These two metrics are mapped for different threshold values in a receiver-operating characteristic (ROC) curve, which illustrates the false alarm rates against true detection rates [Farrar and Worden, 2012].

4 Experimental applications

This section presents two case studies to highlight various aspects of damage detection involving nonlinear and uncertain systems. The first one in subsection 4.1 illustrates a nonlinear magneto-elastic system subjected to linear structural changes and a lower level of data variation related to uncertainties. In this situation, deterministic metrics can be applied. In subsection 4.2, the second one presents an uncertainty-robust damage detection scheme in a magneto-elastic system with nonlinear damage scenarios and a higher level of data variation imposed during the experiments.

4.1 Linear damage detection in a nonlinear magneto-elastic system

The first case study was performed in the MAGNetO-eLastIc beAm (MAGNOLIA[1]) by the SHM Group from UNESP [Shiki et al., 2017]. It was mainly composed of a cantilever aluminum beam with $300 \times 19 \times 3.2$ [mm] and a steel mass attached to its free end. This mass interacted with a permanent neodymium magnet distant 2 [mm] for the steel end in a mono-stable configuration. Similar systems were already investigated in the literature exploring their rich nonlinear behavior in the bi-stable format with multiple magnets [Barton et al., 2010, Erturk and Inman, 2011].

A Modal Shop 2004E electrodynamic shaker was attached 50 [mm] away from the clamped end with a Dytran load cell model 1022V. A Polytec OFV-525/-5000-S laser vibrometer was used to measure the velocity in the beam's free end. A picture of the experimental setup is presented in Figure 3 (a). The nonlinearity in this system comes from the magnetic interactions between the permanent magnet and the steel mass placed in the beam's free end. The magnet is positioned to attract the beam in the axial direction and during the bending movement. Considering the gap of 2 [mm] in this system, a hardening behavior was observed during the experimental tests in this structure. A frequency response curve to a stepped sine input with a shaker-controlled input of 0.01 V and 0.15 V highlights the hardening behavior of the first mode of this system.

Also, a single bolt with 4 nuts (with 2 grams each) was placed in the middle of the beam to simulate mass variations. In this sense, this case study fits the damage detection problems where the structure is nonlinear in the reference state. Still, the Damage was simulated as a simple mass variation that mainly affects linear parameters of this kind of system.

To identify the Volterra model representing the baseline condition of the nonlinear system, a chirp input with two levels: 0.01 and 0.15 V was configured in the shaker to sweep the frequency range from 10 to 50 Hz with 4096 samples acquired with a sampling frequency of 1024 Hz. Figure 4 shows the short Fourier transform of these signals. It is possible to observe the appearance of odd and even harmonics, especially with higher levels of force.

[1]The complete dataset can be obtained on the website of the UNESP SHM Research Group: `https://github.com/shm-unesp/UNESP-MAGNOLIA`

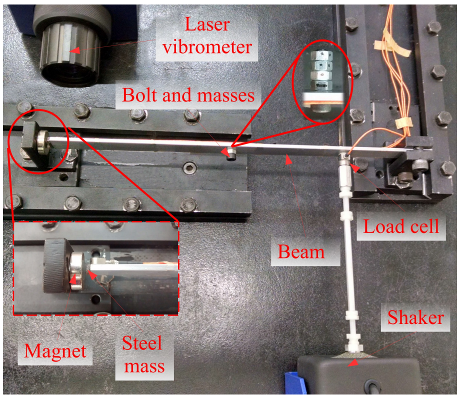

(a) Experimental setup.

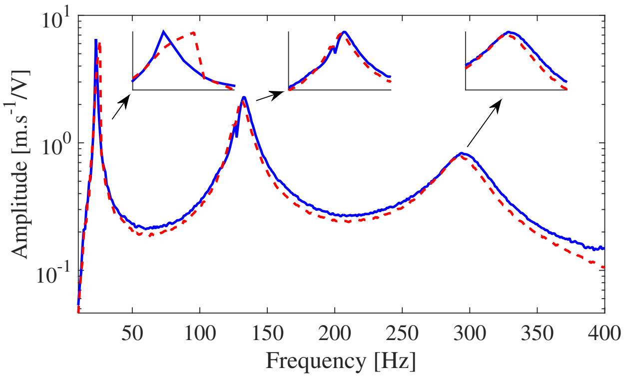

(b) Stepped sine response. ── and - - represents the response to an input of 0.01 V and 0.15 V respectively.

Figure 3: Setup and nonlinear behavior of the MAGNOLIA system.

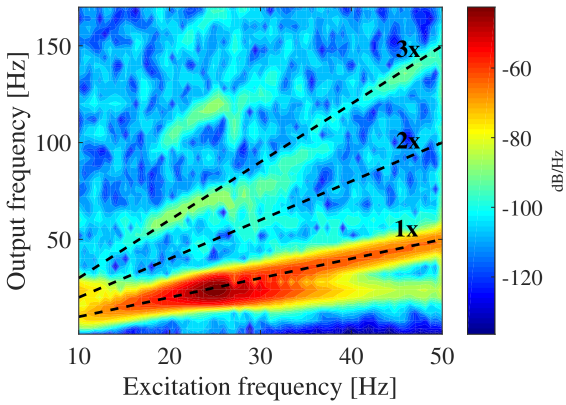

(a) Reference - low amplitude.

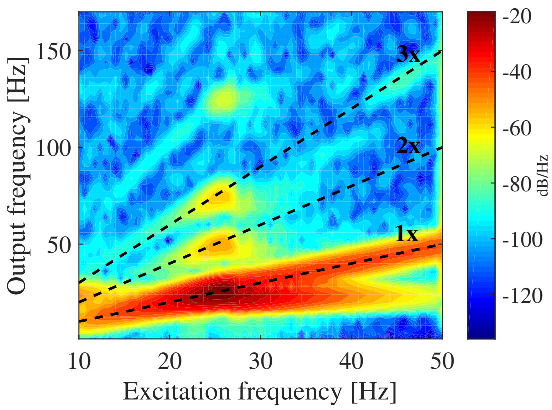

(b) Reference - high amplitude.

Figure 4: Time-frequency representation of the vibration of the MAGNOLIA system under low and high levels of excitation.

With these signals, we identified the Volterra kernels using the procedure described in section 3.1. Since both second and third-order harmonics were detected, the Volterra model was considered to be presented by the first three kernels. A convergence simulation was performed to set the order of the Kautz filters by calculating the prediction error for different model orders. This resulted in the choice of $J_1 = 2$, $J_2 = 2$ and $J_3 = 8$. Figure 5 illustrates the convergence study and the main diagonals of the first three kernels identified to represent the MAGNOLIA system.

The identified model is a nonparametric representation of the MAGNOLIA system in the baseline condition with 4 masses in the bolt in the middle of the structure. To simulate a linear kind of Damage, these masses were removed one by one and placed back in the system simulating the 8 structural states presented in Table 1. The tests for each structural state were repeated 40 times to check the damage indices' repeatability.

Figures 6 and 7 shows the Volterra-based linear and nonlinear damage indices for all the 8 structural conditions using low and high level chirp input. As shown in Figure 4, higher levels of displacement tend to cause stronger nonlinear effects shown by the presence of harmonics in the response. In this sense, the λ_1 linear index shows to be sensitive to the Damage only in the linear

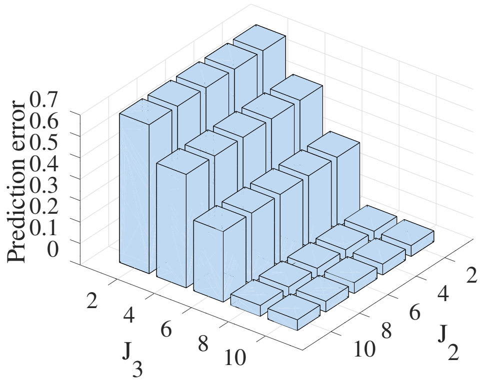

(a) Convergence study of the nonlinear model.

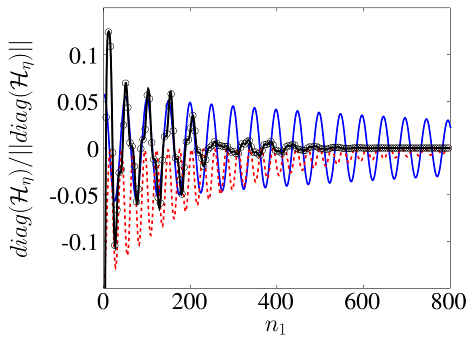

(b) Main diagonal of the Volterra kernels, is the normalized 1^{st} kernel, while and -○- are the normalized main diagonal of the 2^{nd} and 3^{rd} kernel respectively.

Figure 5: Volterra model representing the MAGNOLIA system.

Table 1: Structural states simulated in the MAGNOLIA system.

State	Condition
1	4 masses (baseline)
2	3 masses (damaged)
3	2 masses (damaged)
4	1 mass (damaged)
5	1 mass (repair)
6	2 masses (repair)
7	3 masses (repair)
8	4 masses (repair)

regime of the MAGNOLIA system. Meanwhile, the nonlinear index λ_3 shows to be sensitive to mass variations in both regimes. This simple example clarifies the possible issues when adopting linear damage indicators for monitoring structures with inherent nonlinear behavior.

Tables 2 and 3 illustrate the results of the Volterra-based damage detection for the low and high-level input amplitude for different values of the significance level of the hypothesis test. By the Table 2 it is visible that both λ_1 and λ_3 indexes were able to accurately detect structural variations without any false alarms. However, Table 3 illustrating the results of the nonlinear regime shows that the linear index fails to detect variations while presenting no false alarms. The nonlinear index presents a true high detection for every case, while false alarms can be minimized by using lower values of significance levels.

The behavior of the hypothesis test for different values of significance levels α is illustrated through the ROC curve for both the linear and nonlinear indices. From this analysis, it is clear that the linear indicator can only increase the detection rate through an increase in the false alarm rate during the nonlinear regime of the system. Meanwhile, the nonlinear index presents high values of detection rate without being affected by the nonlinear structural regime.

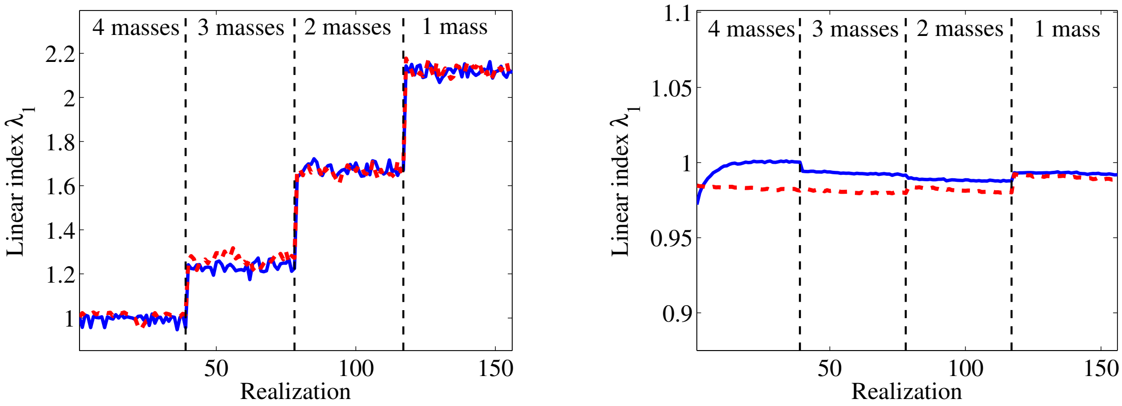

(a) Low level input (0.01 V). (b) High level input (0.15 V).

Figure 6: Linear damage index under two different input levels for the MAGNOLIA system. The continuous line —— represents the indexes during the damage appplications (states 1 to 4) while - - - represents the indexes during the repair (states 5 to 8).

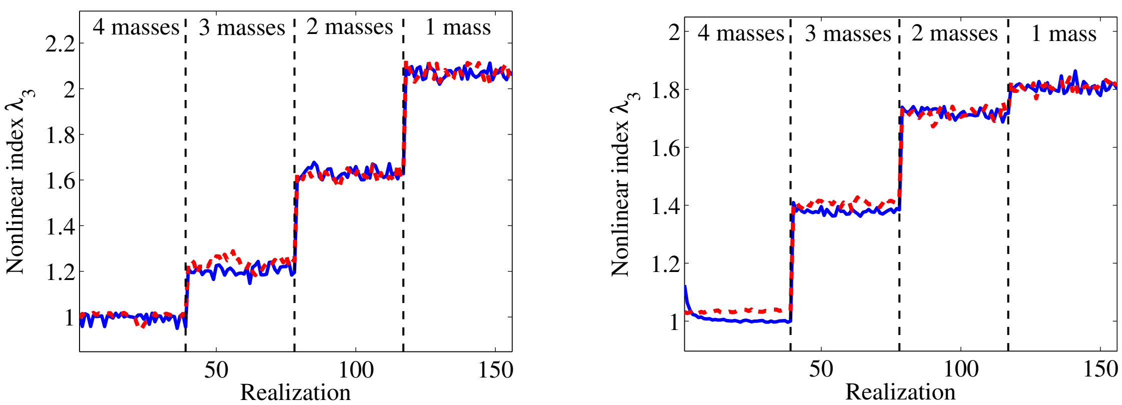

(a) Low level input (0.01 V). (b) High level input (0.15 V).

Figure 7: Nonlinear damage index under two different input levels for the MAGNOLIA system. The continuous line —— represents the indexes during the damage appplications (states 1 to 4) while - - - represents the indexes during the repair (states 5 to 8).

Table 2: Results of the hypothesis tests for different significance levels under low level input (0.01 V) on the MAGNOLIA system.

$\alpha[\%]$	Linear index (λ_1)		Nonlinear index (λ_3)	
	False alarm [%]	True detection [%]	False alarm [%]	True detection [%]
2	0	100	0	100
1	0	100	0	100
0.5	0	100	0	100

Table 3: Results of the hypothesis tests for different significance levels under high level input (0.15 V) on the MAGNOLIA system.

$\alpha[\%]$	Linear index (λ_1)		Nonlinear index (λ_3)	
	False alarm $[\%]$	True detection $[\%]$	False alarm $[\%]$	True detection $[\%]$
2	0	0	34.6	100
1	0	0	17.9	100
0.5	0	0	3.85	100

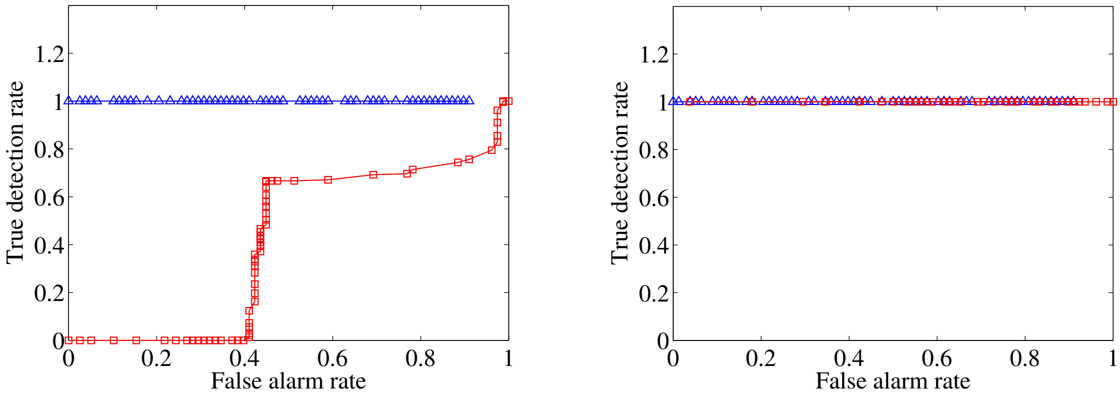

(a) Linear index.

(b) Nonlinear index.

Figure 8: ROC curves of the damage indexes for the MAGNOLIA system. -△- is the curve for the low level input (0.01 V) and -□- is the curve for the high level input (0.15 V).

4.2 Nonlinear damage in a magneto-elastic beam

The second case study was performed in the nonlineAr Damage in a magnEto-eLastic bEam (ADELE[2]) by the SHM Group from UNESP [Villani et al., 2019c]. This is a more challenging benchmark since data variation was induced throughout the experimental tests and the emulated Damage having nonlinear behavior characteristics. The stochastic formulation becomes necessary in this situation to deal with the uncertainties.

The main characteristics of the experimental setup used is presented in Fig. 9, with the structure in the reference condition (without Damage). Figure 9 (a) shows the structure composed of a cantilever beam, constructed by gluing four beams of Lexan together, $2.4 \times 24 \times 240$ [mm^3] each one. At the free boundary, two steel masses are affixed and interact with a magnet, generating a nonlinear behavior in the system response that third-order harmonics can verify in the Time-frequency diagram presented in Fig. 9 (b). The experimental setup uses an Electrodynamic Transducer Labworks Inc. (ET-132) to apply forces to the structure (close to the clamp), an Accelerometer PCB PIEZOTRONICS (352C22) to measure the structure output (close to the free end), and a National Instruments acquisition system to convert and save data. Once again, two levels of input were considered during the experimental tests. A low input amplitude level (1 V RMS) ensures the system oscillates in a linear vibration regime, and a high input amplitude level (6 V RMS) ensures the excitation of the system's nonlinearities.

[2]The complete dataset can be obtained on the website of the UNESP SHM Research Group: https://github.com/shm-unesp/ADELE

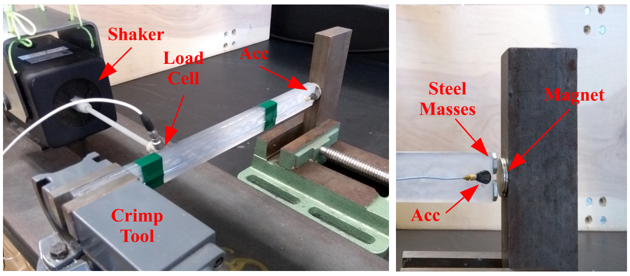

(a) Photos.

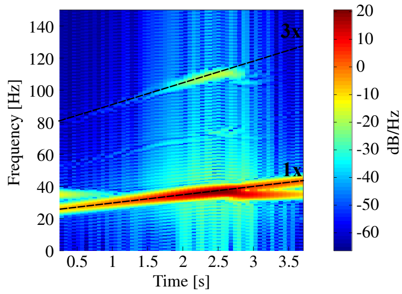

(b) Time-frequency diagram of the system response.

Figure 9: Setup and nonlinear behavior of the ADELE system.

The Damage introduced to the mechanical system aims to simulate a breathing crack behavior. Therefore, four different configurations were constructed:

1. Training beam: 4 intact Lexan beams glued, used to train the model (see Fig. 10 (a));
2. Test beam: 4 intact Lexan beams glued, used to test the model (see Fig. 10 (a));
3. Damage I: 3 intact and 1 cut beams glued (see Fig. 10 (a) and (b));
4. Damage II: 2 intact and 2 cut beams glued (see Fig. 10 (a) and (b));

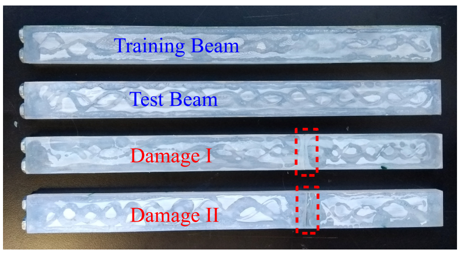

(a) All beams constructed.

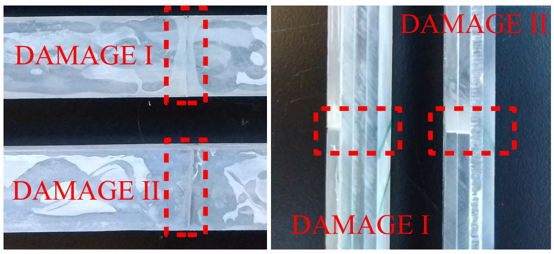

(b) Damaged beams (zoom).

Figure 10: Structural conditions examined.

This kind of structural change can emulate a breathing crack behavior, inducing a nonlinear quadratic behavior in the system that can be verified by observing the results of Fig. 11. The results show that a quadratic harmonic was introduced for the Damage I condition compared with Fig. 9 (b). In contrast, the first and third harmonics are not visually affected. For Damage condition II, all harmonics are altered because of the large extent of Damage.

Furthermore, the data variation was induced by varying the distance between the magnet and the structure. This variation generates great variability in the modal parameters of the structure and of the nonlinear components too. The effect of such variation can be seen in Fig. 1. In this situation, we need to estimate a stochastic model that can represent such variability under reference conditions and separate the nonlinear contributions generated by the presence of the magnet and those generated by the presence of Damage.

For doing so, we can identify a stochastic model using the formulation of Eq. 3, and use this family of models to estimate the indices of Eqs. 7 and 8 that represents the structure in the healthy

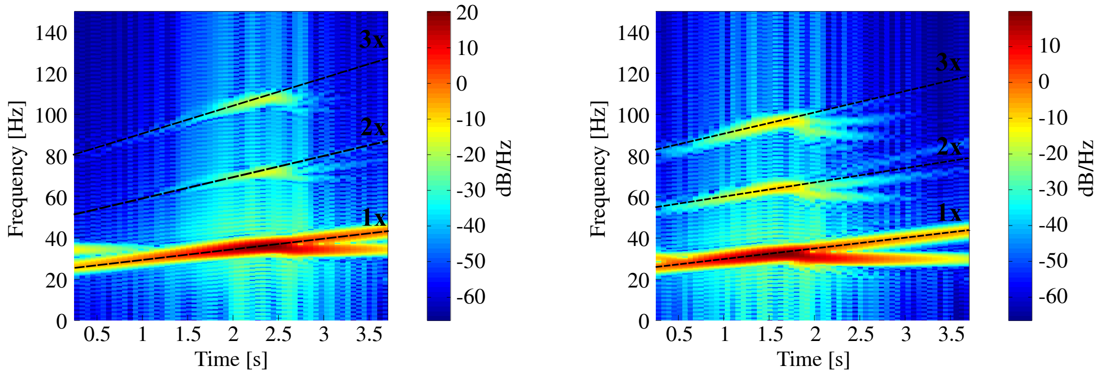

(a) Damage I.

(b) Damage II.

Figure 11: Time-frequency diagram obtained with the structure damaged.

condition. In this step we considered: a chirp input signal varying the excitation frequency from 25 to 40 Hz (first mode shape region) with two levels of amplitude, as mentioned before, $J_1 = 2$, $J_2 = 4$, $J_3 = 6$, and 200 experimental realizations for each structural condition. More information about the step-by-step model estimation procedure can be found in Villani et al. [2019c].

Once the stochastic model is estimated, it can be used to monitor the system. $\mathbb{I}_m$ can be estimated, and in an unknown condition, a new model can be identified to calculate $\mathcal{I}_m$. Finally, the Mahalanobis distance (Eq. 10) is calculated and plotted in Fig. 12 for different structural conditions. It can be noted that the linear index can not detect the nonlinear behavior induced by Damage at the beginning of the propagation (Damage condition I), as expected. When the Damage also changes the linear components (Damage condition II), the linear index values grow. Since the characteristic of the Damage is to induce nonlinear behavior in the structure, the nonlinear index shows an interesting ability to separate the nonlinearities generated by the presence of the magnet from those induced by the presence of the Damage, even at the beginning of the propagation (Damage condition I). Therefore, it is expected that when applying the proposed hypothesis test (Eq. 15) the nonlinear index will show a more robust behavior, even considering the variability of the data.

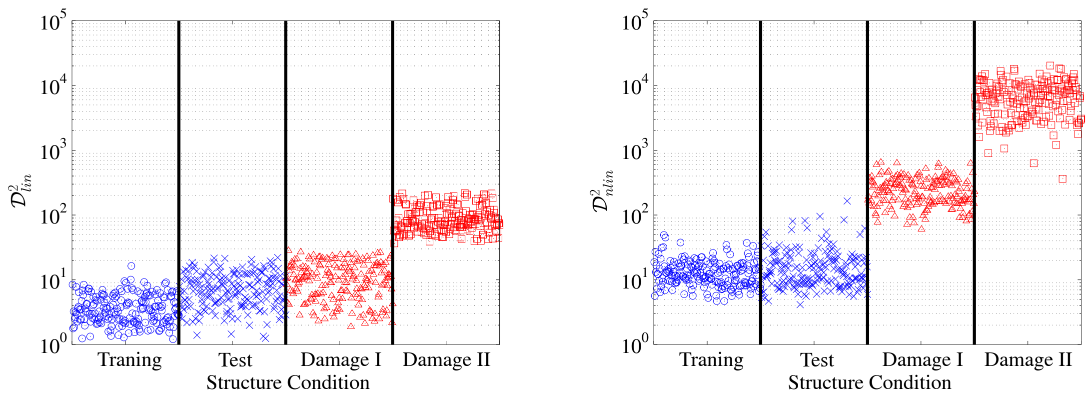

(a) Linear index.

(b) Nonlinear index.

Figure 12: Evolution of the Mahalanobis distance.

Table 4 shows the results obtained for both linear and nonlinear indices when applying the

Table 4: **Hypothesis test results for ADELE system.**

	ϵ	False detection [%]		True detection [%]	
		Training Beam	Test Beam	Damage I	Damage II
Linear Index	10^{-2}	0.5	15.5	34.5	100
	10^{-4}	0	0	5	100
	10^{-6}	0	0	0	100
	10^{-12}	0	0	0	75
Nonlinear Index	10^{-2}	4.5	12.5	100	100
	10^{-4}	1	7	100	100
	10^{-6}	0	4.5	100	100
	10^{-12}	0	1.0	96.5	100

hypothesis test. The test is applied using various values for the sensitivity (ϵ). Despite presenting a higher level of false positives because of its high sensitivity, the nonlinear index has a considerably better performance in detecting this type of Damage, even considering the great variability of the data. It is worth remembering that a false positive error can generate less catastrophic consequences than a false negative error, as is seen in the case of the linear index. This ratio between false positives and false negatives could be controlled by choosing the value of ϵ optimally, depending on the level of reliability and cost that the error may cause in each practical application.

Finally, we can study the degree of separability of the data that these indices generate by varying the sensitivity of the hypothesis test and constructing the ROC curve. Figure 13 shows the results obtained. The results revealed that monitoring the nonlinear components of the structure output signal, depicted by the second and third-order kernel coefficients and contributions used to fill the feature vector, is an interesting methodology to be deployed in damage detection problems, mainly when the Damage exhibits nonlinear characteristics. Additionally, when data variation represents an issue, the use of the stochastic reference model can improve the capability of the method to distinguish the changes related to the presence of Damage from the ones related to the presence of uncertainties. Knowing that the closer to the point (0,1), the better the index's performance, we can conclude that the nonlinear index performed better.

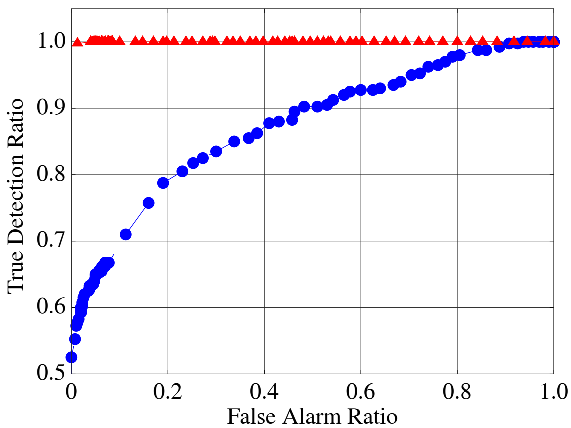

Figure 13: ROC curves of the damage indexes for ADELE system. ○ represents the linear index and △ represents the nonlinear index.

5 Final Remarks

This chapter has demonstrated by some simple illustrative examples how nonlinear vibration and operation regimes with parameter uncertainty can compromise the correct diagnosis of the structural state of a system. Some methods of dealing with these difficulties were presented based on systems identification techniques that seek to filter linear and nonlinear components in a stochastic way and group the effects according to their causes and effects. The results confirmed that the procedure's robustness is increased when both effects are mitigated.

It is evident that when not assumed, the possibility of propagating uncertainties and identifying and separating the nonlinear behavior from damage and operation confounded the detection. On the other hand, these techniques demand more knowledge from the SHM engineer to identify these sources and the requirement of implementing some strategy to allow the correct classification.

Acknowledgements

The authors gratefully acknowledge, for the financial support given to this research, the following Brazilian agencies: Coordenação de Aperfeiçoamento de Pessoal de Nível Superior (CAPES) - Finance Code 001; São Paulo Research Foundation (FAPESP), grant numbers 12/09135-3, 13/25148-0, 15/25676-2, 17/24977-4 and 19/19684-3; Brazilian National Council for Scientific and Technological Development (CNPq) grant number 306526/2019-0 ; and Fundação Carlos Chagas Filho de Amparo à Pesquisa do Estado do Rio de Janeiro (FAPERJ) grants 210.167/2019, 211.037/2019 and 201.294/2021.

References

D. Barton, S. Burrow, and L. Clare. Energy harvesting from vibrations with a nonlinear oscillator. *ASME Journal of Vibrations and Acoustics*, 132(2):021009, 2010. doi: 10.1115/1.4000809.

J. Bendat and A. Piersol. *Random Data: Analysis and Measurement Procedures*. Wiley Series in Probability and Statistics. Wiley, 2011. ISBN 9781118210826. URL `https://books.google.com.br/books?id=qYSViFRNMlwC`.

L. Bornn, C. R. Farrar, and G. Park. Damage detection in initially nonlinear systems. *International Journal of Engineering Science*, 48(10):909–920, 2010. ISSN 0020-7225. doi: 10.1016/j.ijengsci.2010.05.011. URL `http://www.sciencedirect.com/science/article/pii/S0020722510001059`. Structural Health Monitoring in the Light of Inverse Problems of Mechanics.

A. Cunha Jr, R. Nasser, R. Sampaio, H. Lopes, and K. Breitman. Uncertainty quantification through Monte Carlo method in a cloud computing setting. *Computer Physics Communications*, 185:1355–1363, 2014. doi: https://doi.org/10.1016/j.cpc.2014.01.006.

S. da Silva, S. Cogan, and E. Foltête. Nonlinear identification in structural dynamics based on Wiener series and Kautz filters. *Mechanical Systems and Signal Processing*, 24(1):52–58, Jan. 2010. ISSN 0888-3270. URL `http://www.sciencedirect.com/science/article/pii/S0888327009001897`.

A. Erturk and D. Inman. Broadband piezoelectric power generation on high-energy orbits of the bistable duffing oscillator with electromechanical coupling. *Journal of Sound and Vibration*, 330(10):2339 – 2353, 2011. ISSN 0022-460X. doi: http://dx.doi.org/10.1016/j.jsv.

2010.11.018. URL http://www.sciencedirect.com/science/article/pii/S0022460X10007807. Dynamics of Vibro-Impact Systems.

C. R. Farrar and K. Worden. *Machine Learning and Statistical Pattern Recognition*, pages 295–320. John Wiley & Sons, Ltd, 2012. ISBN 9781118443118. doi: 10.1002/9781118443118.ch9. URL http://dx.doi.org/10.1002/9781118443118.ch9.

M. Ghrib, M. Rébillat, G. V. des Roches, and N. Mechbal. Automatic damage type classification and severity quantification using signal based and nonlinear model based damage sensitive features. *Journal of Process Control*, 2018. ISSN 0959-1524. doi: https://doi.org/10.1016/j.jprocont.2018.08.002. URL http://www.sciencedirect.com/science/article/pii/S0959152418301975.

G. Grimmett and D. Welsh. *Probability: an introduction*. Oxford University Press, 2014.

W. H. Kautz. Transient synthesis in the time domain. *Circuit Theory, Transactions of the IRE Professional Group on*, CT-1(3):29–39, September 1954. ISSN 0197-6389. doi: 10.1109/TCT.1954.1083588.

G. Kerschen, K. Worden, A. F. Vakakis, and J.-C. Golinval. Nonlinear system identification in structural dynamics: current status and future directions. In *25th International Modal Analysis Conference, Orlando, 2007*, 2007.

D. P. Kroese, T. Taimre, and Z. I. Botev. *Handbook of Monte Carlo Methods*. Wiley, 2011.

J. M. Nichols and M. D. Todd. *Nonlinear Features for SHM Applications*. American Cancer Society, 2009. ISBN 9780470061626. doi: 10.1002/9780470061626.shm049. URL http://onlinelibrary.wiley.com/doi/abs/10.1002/9780470061626.shm049.

Z. Peng, J. Li, H. Hao, and C. Li. Nonlinear structural damage detection using output-only volterra series model. *Structural Control and Health Monitoring*, 28(9):e2802, 2021. doi: https://doi.org/10.1002/stc.2802. URL https://onlinelibrary.wiley.com/doi/abs/10.1002/stc.2802.

M. Rébillat, R. Hajrya, and N. Mechbal. Nonlinear structural damage detection based on cascade of Hammerstein models. *Mechanical Systems and Signal Processing*, 48(1):247–259, 2014. ISSN 0888-3270. doi: http://dx.doi.org/10.1016/j.ymssp.2014.03.009. URL http://www.sciencedirect.com/science/article/pii/S0888327014000843.

M. Schetzen. *The Volterra and Wiener Theories of Nonlinear Systems*. Wiley, 1980.

S. B. Shiki, S. da Silva, and M. D. Todd. On the application of discrete-time Volterra series for the damage detection problem in initially nonlinear systems. *Structural Health Monitoring*, 16(1):62–78, 2017. doi: 10.1177/1475921716662142. URL http://dx.doi.org/10.1177/1475921716662142.

H. Sohn and C. R. Farrar. Damage diagnosis using time series analysis of vibration signals. *Smart Materials and Structures*, 10(3):446–451, jun 2001. doi: 10.1088/0964-1726/10/3/304. URL https://doi.org/10.1088/0964-1726/10/3/304.

C. Soize. *Stochastic models of uncertainties in computational mechanics*. Amer Society of Civil Engineers, 2012.

C. Soize. *Uncertainty Quantification: An Accelerated Course with Advanced Applications in Computational Engineering*. Springer, 2017.

L. G. G. Villani, S. da Silva, and A. Cunha Jr. Damage detection in uncertain nonlinear systems based on stochastic Volterra series. *Mechanical Systems and Signal Processing*, 125:288–310, 2019a. ISSN 0888-3270. doi: https://doi.org/10.1016/j.ymssp.2018.07.028. URL http://www.sciencedirect.com/science/article/pii/S0888327018304291. Exploring nonlinear benefits in engineering.

L. G. G. Villani, S. da Silva, A. Cunha Jr, and M. D. Todd. Damage detection in an uncertain nonlinear beam based on stochastic Volterra series: An experimental application. *Mechanical Systems and Signal Processing*, 128:463–478, 2019b. ISSN 0888-3270. doi: https://doi.org/10.1016/j.ymssp.2019.03.045. URL http://www.sciencedirect.com/science/article/pii/S0888327019302250.

L. G. G. Villani, S. da Silva, A. Cunha Jr, and M. D. Todd. On the detection of a nonlinear damage in an uncertain nonlinear beam using stochastic Volterra series. *Structural Health Monitoring*, 2019c. doi: 10.1177/1475921719876086. URL http://doi.org/10.1177/1475921719876086.

K. Worden, G. Kerschen, A. F. Vakakis, and J.-C. Golinval. Nonlinear System Identification in Structural Dynamics: A Short (and Biased) History. In *25th International Modal Analysis Conference, Orlando, 2007*, pages 1996–2017, 2007.

X. Xia, J. Zhou, J. Xiao, and H. Xiao. A novel identification method of Volterra series in rotor-bearing system for fault diagnosis. *Mechanical Systems and Signal Processing*, 66-67:557–567, 2016. ISSN 0888-3270. doi: https://doi.org/10.1016/j.ymssp.2015.05.006. URL http://www.sciencedirect.com/science/article/pii/S0888327015002277.

M. Yeager, B. Gregory, C. Key, and M. Todd. On using robust Mahalanobis distance estimations for feature discrimination in a damage detection scenario. *Structural Health Monitoring*, 18(1): 245–253, 2019. doi: 10.1177/1475921717748878. URL https://doi.org/10.1177/1475921717748878.